Electronic Supplementary Material (ESI) for Journal of Materials Chemistry B.

Cryoablation-Activated Enhanced Nanodoxorubicin Release for the Therapy of Chemoresistant Mammary Cancer Stem-like Cells

Yi Hou [a,b,c†], Xuyang Sun [a,b†], Siyuan Yao [a,b], Wei Rao [a,b,c,*], Xiaoming He [d,e,f]

[a] CAS Key Laboratory of Cryogenics, Technical Institute of Physics and Chemistry, Chinese Academy of Sciences, Beijing 100190, China
[b] Beijing Key Laboratory of Cryo-Biomedical Engineering, Technical Institute of Physics and Chemistry, Chinese Academy of Sciences, Beijing 100190, China
[c] School of Future Technology, University of the Chinese Academy of Sciences, Beijing 100049, China
[d] Fischell Department of Bioengineering, University of Maryland, College Park, MD, USA
[e] Department of Biomedical Engineering, The Ohio State University, Columbus, OH 43210, USA
[f] Comprehensive Cancer Center, The Ohio State University, Columbus, OH 43210, USA

[†] Equal contribution.

*Corresponding author: Wei Rao. E-mail: weirao@mail.ipc.ac.cn .Tel. +86-10-82543719. Fax: +86-10 82543766

Table S1. Encapsulation efficiency (EE) and loading content (LC) at different feeding ratios of free doxorubicin (fDOX) to Pluronic F127-chitosan NPs in weight and the diameter of the resultant GNPs-encapsulated doxorubicin (gnDOX) determined by dynamic light scattering (DLS) at different temperature. Also shown are the data of size for empty GNPs.

Feeding ratio fDOX : NPs	EE, %	LC, %	Diameter of GNPs/gnDOX, nm		
			DI		
			4 °C	22 °C	37 °C
0 : GNPs	N/A	N/A	113.4 ± 8.5	82.2 ± 4.6	37.3 ± 2.2
1 : 50	54.5 ± 3.0	1.1 ± 0.1	46.0 ± 4.9	33.7 ± 1.0	31.0 ± 5.5
1 : 20	49.0 ± 4.1	2.5 ± 0.2	54.7 ± 7.7	43.1 ± 9.0	31.1 ± 3.5
1 : 10	33.8 ± 2.7	3.4 ± 0.3	127.0 ± 6.4	98.5 ± 9.4	55.2 ± 8.9

All data are presented as mean ± standard deviation and N/A represents " not applicable".

Table S2. Encapsulation efficiency (EE) and loading content (LC) of doxorubicin (DOX) with and without genipin crosslinking.

Feeding ratio DOX : NPs	Genipin crosslinking	EE, %	LC, %
1 : 10	No	9.9 ± 0.9	0.2 ± 0.0
1 : 10	Yes	33.8 ± 2.7	3.4 ± 0.3

NPs: Pluronic F127-chitosan nanoparticles

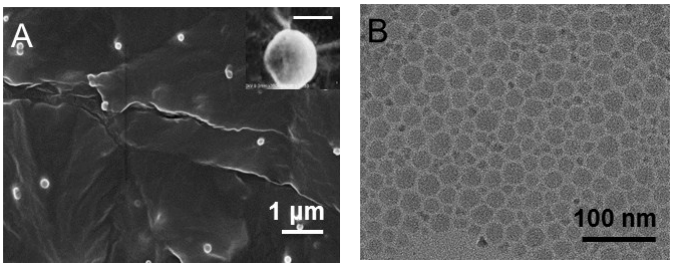

Figure S1. (A) A typical SEM image of GNPs showing their spherical morphology and nanoscale sizes at 22 °C. The scale bar is 50 nm. (B) A typical TEM image of GNPs showing their core shell morphology and nanoscale sizes at 22 °C.

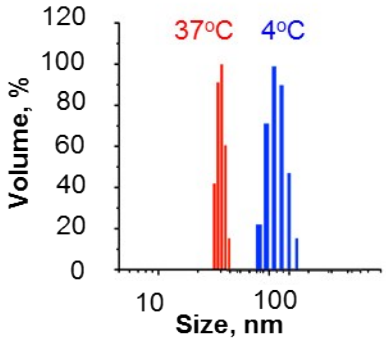

Figure S2. Typical dynamic light scattering (DLS) results showing the size of gnDOX when dissolved in deionized water at 37 °C and 4 °C and the thermal responsiveness characteristics.

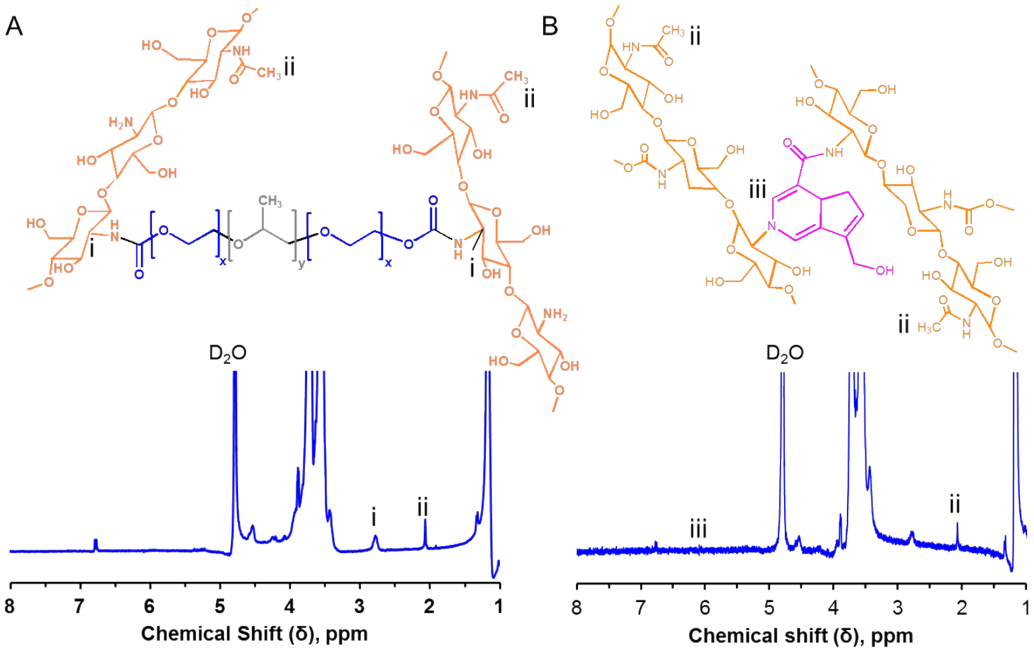

Figure S3. (A) Typical ^{1}H NMR spectra of Pluronic F127-chitosan shows the successful crosslink formation of Pluronic F127-chitosan. Two characteristic peaks of chitosan at δ~2.7 (i, for protons in chitosan on C2 carbon linked to the amide bond between Pluronic F127 and

chitosan) and 2.0 ppm (ii, for protons in the 5% residual methyl groups of chitosan) appeared in the spectra. (B) Typical ^{1}H NMR spectra of GNPs showing a characteristic peak (iii) of genipin.

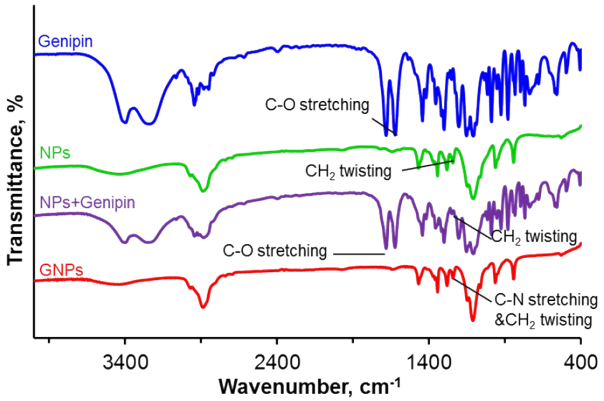

Figure S4. Typical FTIR spectra of genipin (GP), Pluronic F127-chitosan nanoparticles (NPs), a simple mixture of Pluronic F127-chitosan NPs, and GP (NPs + GP), and GNPs showing changes in characteristic peaks as a result of the cross-linking reaction between genipin and chitosan.

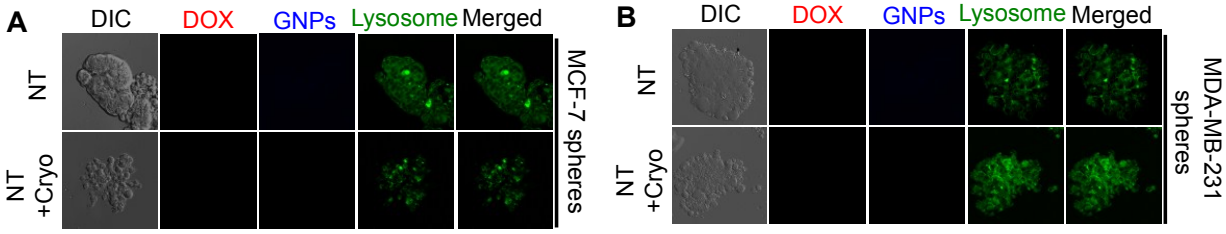

Figure S5. Micrographs showing no DOX red fluorescence in mammosphere cells treated with no treatment (NT) as controls, together with or without cryoablation treatment. (A) Micrographs in MCF-7 mammosphere cells. (B) Micrographs in MDA-MB-231 mammosphere cells.

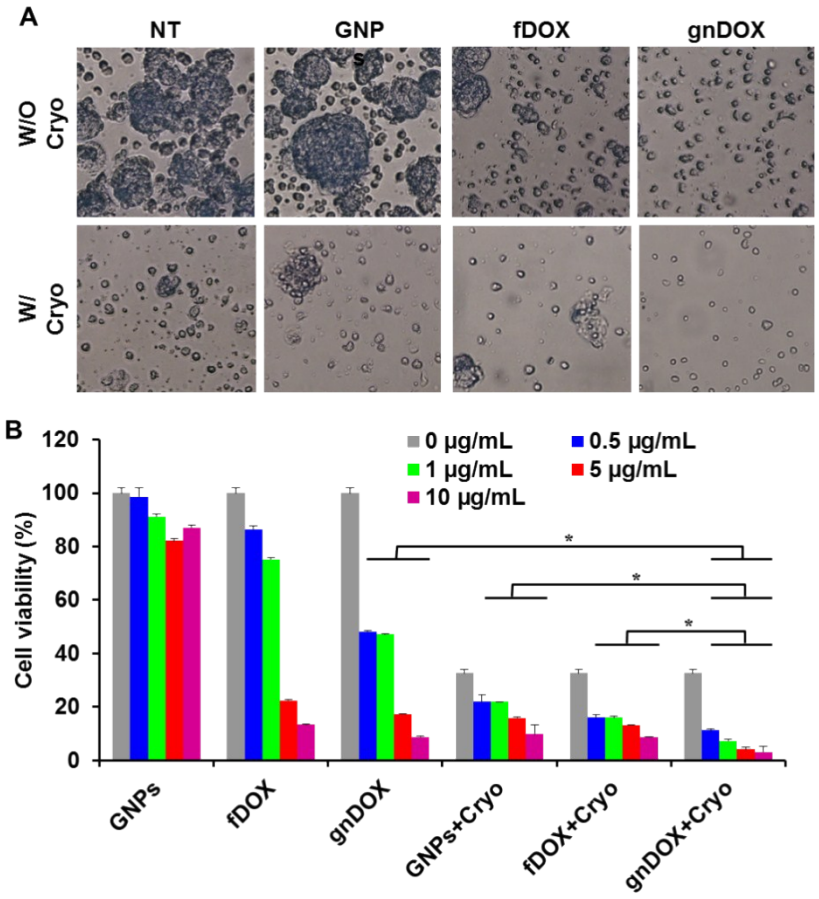

Figure S6. Morphologic and quantitative cell viability data of mammosphere cells showing the combined treatment of cryoablation and gnDOX is significantly more effective than cryoablation alone, gnDOX alone or combination of cryoablation and fDOX in destroying the 4T1 mammosphere cells. (A) Typical micrographs showing morphologic survival of the 4T1 mammosphere cells and (B) Quantitative cell viability data after various treatments of 4T1 mammosphere cells and. *: $p < 0.05$.

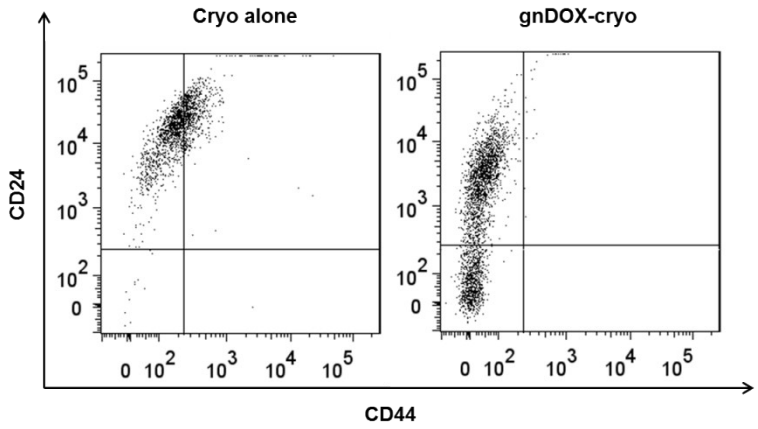

Figure S7. Analysis of CD44 and CD24 expression in vitro after treatment showing gnDOX combined with cryoablation reducing the expression of CD44.

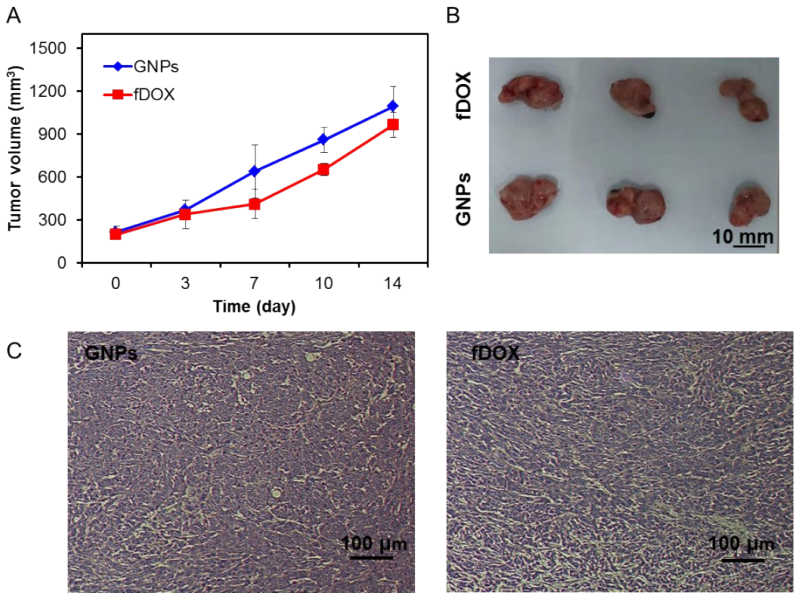

Figure S8. In vivo antitumor capacity of GNPs and fDOX. (A) Tumor growth curves for GNPs and free DOX treatments showing no obvious tumor elimination capacity. (C) Images of tumors on day 14 after the first treatment for GNPs and fDOX. (D) Representative micrographs of hematoxylin and eosin (H&E) staining of tumors showing no significant difference and tumor elimination of GNPs and fDOX treatments.

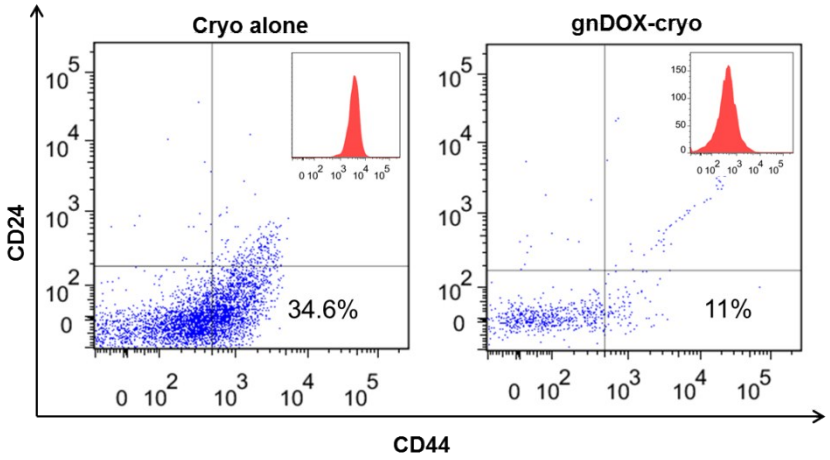

Figure S9. Analysis of CD44 and CD24 expression in vivo after treatment showing that gnDOX combined with cryoablation reduces the expression of CD44 which reduces the stemness of mammosphere cells including CSLCs.

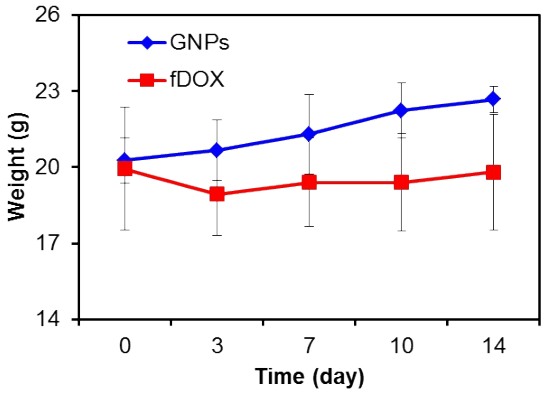

Figure S10. Body weight curves of mice showing no significant toxicity of GNPs treatment group and slight toxicity of fDOX in the first three days.

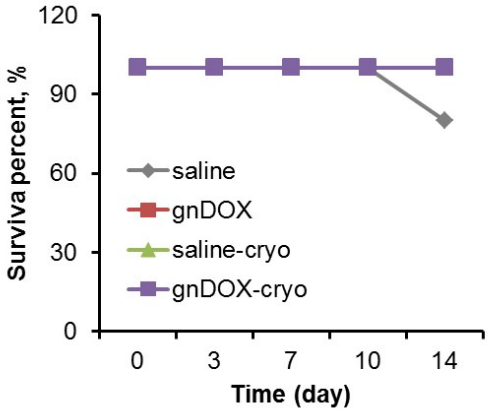

Figure S11. Animal survival after different treatments showing that no mice with treatment of gnDOX, saline-cryo, or gnDOX-cryo died.